

Proposal to Place Wavelength-shifting Reflector Foils on the SBND Cathode Plane Assembly

A. M. Szelc¹, D. Garcia-Gomez¹, C. Hill¹, V. Basque¹, F. Spagliardi¹, A. Furmanski¹, E. Segreto², A. A. Bergamini-Machado³, B. Littlejohn⁴, D. Martinez-Caicedo⁴, and F. Cavanna⁵

¹University of Manchester

²UNICAMP + UFABC

³UFABC

⁴Illinois Institute of Technology

⁵Fermilab

September 26, 2017

Abstract

In this document we propose to manufacture and install 128 di-electric foils evaporated with wavelength-shifting Tetraphenyl butadiene in the SBND Cathode Plane Assembly (CPA). These new components of the SBND Photon Detection System (PDS) will greatly improve the uniformity of light collection which translates into improved calorimetric reconstruction using scintillation light as well as improved timing resolution. The installed foils combined with the choice to leave a few PMTs uncovered enables a new feature in LArTPCs, namely positional resolution in the drift coordinate using scintillation light only, which will improve background rejection from cosmic events. A similar setup to the one proposed has been operated in the LArIAT detector, demonstrating long term stable operation in a LArTPC running in a beamline. In this document we present the benefits of installing the foils, the R&D performed to ensure the successful installation as well as the production procedure and the resources necessary to perform the production.

1 Introduction

Liquid Argon Time Projection Chamber detectors are quickly becoming the state of the art in neutrino detectors. The currently only approved long-baseline neutrino experiment, DUNE, will be using liquid argon technology. In the framework of the US-based neutrino programme, in a relatively short time, these detectors have had to evolve from small chambers like ArgoNeuT to mid-size chamber like MicroBooNE and SBND to extremely large-scale projects like DUNE. This has necessitated a focus on development of engineering solutions for these larger scale detectors leaving somewhat less resources to improve the technology itself. One area that in our opinion has not been fully exploited is the collection of scintillation light emitted by the argon. LArTPCs at neutrino energies are focused on charge collection with wire planes and have mostly used scintillation light as a trigger [10]. MicroBooNE [6] has developed techniques to use scintillation light to reject cosmic ray backgrounds or, more precisely, to identify the neutrino interaction in the TPC through the shape of the light signal. The full potential of scintillation light in liquid argon neutrino detectors has still not been tapped. Scintillation light can be used to enhance the performance of liquid argon detectors in neutrino physics in several ways: the most obvious ones being energy reconstruction, timing, position reconstruction and triggering.

One of the goals of the Short Baseline Near Detector (SBND) is to develop the liquid argon technology in addition to its rich physics programme. From the beginning, one of the main areas of this R&D has been scintillation light, and one of the options has been installing WLS-covered reflector foils to enhance light collection. The aim of this potential new detector element was to develop light collection technology for future large scale detectors. This proposal aims to fulfil

this idea by proposing to prepare a set of TPB evaporated di-electric foils and install them on the cathode plane assembly (CPA) of the SBND detector. The foils will be coated with the wavelength shifter at dedicated production sites at Manchester and Campinas, after the substrates will have been prepared at IIT in Chicago. The samples would then be installed in the SBND CPA and held together by two layers of metallic mesh. This will enable the SBND light collection system to reap the benefits of the enhanced light collection, without affecting the electric field used in the TPC. The components and labour will be funded by the Manchester, UNICAMP and IIT groups.

Di-electric foils evaporated with WLS compounds have been used in several experiments, primarily at Dark Matter recoil energies, [14, 9] but also at neutrino energies - [15]. We have experience in running detectors with such a setup, as well as manufacturing large quantities of such foils.

This document is organized as follows: in Section 2 we present the motivation to install the foils in SBND, focusing on applications in timing and calorimetry. We give an overview of the results of the detailed simulation designed and used to understand the performance of the Photon Detection System with the addition of wavelength shifter covered foils on the cathode. In Sec. 3 we present the technical details of the foils, their preparation and proposed installation method. In Sec. 4 we discuss the resources needed to complete the production. Finally in Sec. 5 we report on R&D activities we performed to ensure the robustness of this solution.

2 Motivation

As mentioned previously, we believe that scintillation light is essential to improving the performance of liquid argon neutrino detectors. The clearest improvement can be obtained at lowest energy interactions. It is expected that supernova energy reconstruction could be improved significantly by combining charge collection and scintillation light. The augmented light collection efficiency and positional resolution can also improve cosmic background rejection and energy reconstruction of beam neutrino events below 200MeV, especially Electro-Magnetic showers. This has not been yet quantified, although dedicated studies with the LArIAT data are starting.

2.1 Low Energy Neutrinos (Supernova + Low Energy EM Showers)

Liquid argon detectors are mostly sensitive to neutrinos and not anti-neutrinos from supernovae. This makes them unique in the field and the prospect to detect supernova neutrinos in DUNE (or other liquid argon detectors) so compelling. Supernova neutrinos can provide crucial information about mass-ordering[26] as well as the still not understood processes that govern the supernova explosion [22]. In case of a galactic-centre core-collapse supernova, SBND is likely to see on the order 10-20 neutrino events in the course of few seconds in total.

Given the low energy of supernova neutrino events and the overwhelming amount of backgrounds it is currently not expected that SBND will be able to trigger on these neutrinos, and instead will rely on a trigger from the SNEWS warning network[12]. This is especially true in case of a non-uniform light collection expected in the baseline system. In this case even low energy events from ^{39}Ar close to the PMTs can have a signature comparable to neutrino events with 10x higher energies. This makes it difficult to apply reasonable cuts to reject radioactive backgrounds while keeping the interesting part of the signal. A uniform light collection system improves this significantly, see Sec.5.3 and [16] for a more thorough discussion. These studies show that it might be possible to implement selection cuts for events in the interesting range, as the scintillation yield becomes translatable to energy.

In order to extract information from supernova neutrinos, excellent energy reconstruction is needed. Charge reconstruction has been found to work reasonably well, [7], however it is not clear that the resolution obtained there is sufficient to differentiate between different supernova models. Even this reconstruction assumes a perfect identification of each charge energy deposition with the time at which it occurred in the event frame. If this condition is not fulfilled the charge losses from impurities cannot be corrected for and the resolution will be worse. Interestingly, scintillation light itself provides an additional method of reconstructing energy. This has been demonstrated by the LArIAT experiment, which used light to reconstruct the energy spectrum of Michel electrons, shown in Fig. 1. One should note, that this was possible thanks to WLS covered foils installed inside the fieldcage. The resolution is comparable to that of charge and as the two mechanisms of expression of deposited energy are anticorrelated it is expected that their combination will provide

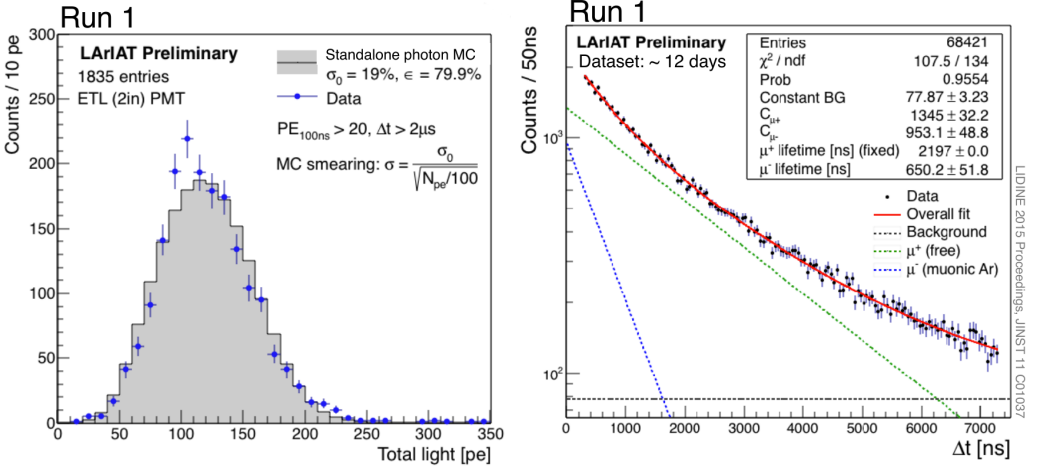


Figure 1: Michel energy spectrum reconstructed using scintillation light in the LArIAT detector [18].

a better energy resolution, in a way analogous to that demonstrated by the EXO-200 experiment for liquid xenon. These studies are being finalized with the LArIAT data.

The enhancement from using scintillation will increase the precision of energy reconstruction of higher energy events. This should be especially beneficial in case of EM-showers, as a fraction of their energy is carried away by low energy gammas, which can Compton scatter and pair produce in the detector. In both cases these energy depositions can occur far away from the shower body and result as not clustered by charge reconstruction algorithms. In addition, these energy depositions can be too small to be registered by hit-finding algorithms even when they are close by. In both cases the scintillation light can improve the situation as even low energy depositions should contribute to the glow of light associated with the shower, and the timing cut will ensure including even spatially far away scatters. The resulting improvement in the energy reconstruction of beam electron neutrinos, will lead to a more precise prediction of the un-oscillated neutrino flux at SBND, improving the unoscillated flux predictions at MicroBooNE and ICARUS. It is difficult to quantify the improvement of using scintillation light to aid the energy reconstruction of EM showers, given that the exact energy resolution for reconstructing EM-showers using charge is still being determined by e.g. MicroBooNE. A set of LArIAT electron events, containing charge and scintillation light information is being selected and will be studied in the future to try to understand this performance.

2.2 Simulations of the Effects of Installing Foils on the SBND Cathode

The expected benefits of installing the WLS-covered foils in SBND are based on the detailed simulation performed in the SBND geometry using the LArSOFT software package. The full details of the simulation can be found in SBN-DocDB#1155 [20], however, we will mention a few highlights in this section.

2.2.1 Uniformity and Energy Reconstruction

The primary advantage of installing WLS-covered reflector foils is the recovery of uniformity of light collection in the detector. An illustrative plot is shown in Fig. 2 (left). The re-emitted, and reflected visible component (red) is complementary to the direct VUV (blue) and as a result their sum is relatively uniform along the drift direction. In the baseline design the same energy can result in an amount different by an order of magnitude depending on where the deposition happens. This makes designing a precise trigger for low energy events (and backgrounds) based on scintillation light more complicated. See Sec. 5.3, and especially, [16], for a discussion of the enhancement of low background rejection with scintillation light.

Liquid Argon scintillation light has been successfully used for calorimetric purposes in Dark Matter detectors, as well as at Michel electron energies - Fig. 1. The possibility to use scintillation light to augment charge-based energy reconstruction is under study, e.g. using LArIAT data, but

simulations can already provide some input. Fig. 2 (right) shows the variation in light collected (which can be translated to energy resolution) from simulated proton tracks. For the visible and VUV components (red and blue) the resolution gets worse with higher energy, which seems counter-intuitive. This is an effect of non uniformity of the light collection. The protons used for the plot were shot an angle of 10 degrees off of the beam axis. The higher the energy, the further the protons traverse to regions with a different collection efficiency which leads to a different detector response along the path and therefore larger fluctuations and lower energy resolution. Using a sum of both light components (black) compensates for this effect and recovers reasonable uniformity.

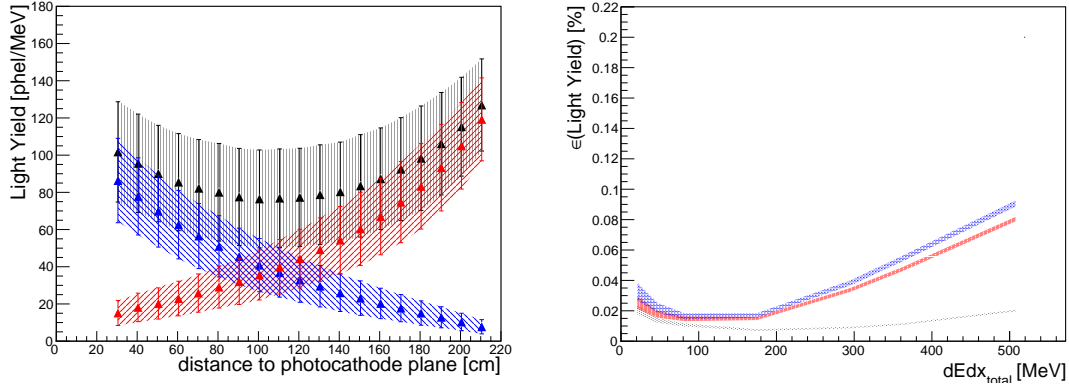


Figure 2: (Left) Light yield in the detector for the direct (blue), reflected and reemitted (red) and total (black) light components. The bands account for geometric effects along the edges of the TPC. (Right) Relative uncertainty in the light yield for proton tracks shot at a 10 degree angle from the cathode plane, calculated as the ratio of the RMS and the mean of the histogram of number of detected photons for a given sample, colors as previously. [20]

2.2.2 Effects on Timing

The SBND light detection system simulations have shown that the main factor affecting time resolution is the width of the argon light emission peak itself combined with the steep growth of the refractive index at VUV wavelengths which translates into large differences of velocities despite the relatively narrow emission peak in argon. These two facts mean that the direct VUV light emitted by liquid argon will arrive relatively late and with a dispersion growing with the distance from the optical detectors as can be seen in Figure 3 (blue points). This effect can be mitigated if the light is quickly wavelength shifted to the visible range. Figure 3 shows the dispersion of photon arrival times for the direct VUV¹ light (blue) and wavelength-shifted light reflected off of the cathode walls (red) in SBND. The two populations are compared based on the expected photon arrival time. It can be seen that a LDS able to collect the direct and the re-emitted light components would allow maintaining a resolution of a few nanoseconds throughout the whole active volume, if the PMTs and electronics maintain similar precision. Such resolution will be extremely beneficial for searches for exotic particles, such as so-called Dark Sector particles and Heavy Sterile Neutrinos. More importantly it could allow observing the beam bucket structure of the Booster Neutrino Beam leading to a higher background rejection rate for beam events.

2.2.3 Position Reconstruction

An extremely important aspect of running a LArTPC on the surface, as demonstrated by MicroBooNE [6], is the ability to reconstruct position using scintillation light. This feature is essential to match the multiple charge depositions present in a given readout frame with their arrival times. This matching is needed to properly reconstruct the drift time and therefore position in the drift coordinate - x. More importantly, it enables identifying the track or EM-shower activity that corresponds to the neutrino beam-gate, greatly enhancing background rejection. Fig. 4 shows that such position reconstruction is possible in the SBND detector with installed foils. In fact, the large

¹Note that the VUV direct light, to be detected, will be wavelength shifted into the visible spectrum by the TPB coating the PMT window, and re-emitted with a forward efficiency of 50%.

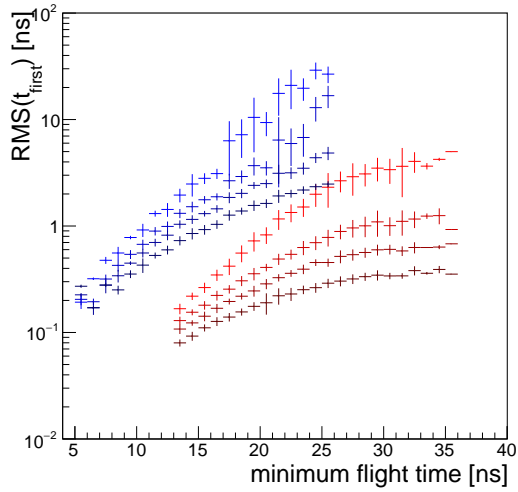


Figure 3: Reconstructed "PMT time resolution" for point-like sources and the different light components, VUV (blue), visible (red), in the configurations under study. The profiles represent the spread (RMS) of the first arrival time (t_{first}) in the PMTs, as a function of the minimum time of flight, given a scintillation point. Note that for the VUV light this translates as direct distance from energy deposition, which is not the case for the visible component where the time corresponds to the shortest path of the reflected light to the PMT. The four profiles have been calculated for 25, 75, 200 and 1000 MeV energy deposited in the liquid argon, improving the resolution with the energy (from lighter to darker), as expected [20].

number of PMTs installed in SBND enables attempting to fit the track direction and end-points using only scintillation light. This in itself shows that the presence of re-emitted light coming from foils on the cathode does not wash out position reconstruction in the y-z plane and that the system should be capable of "flash-matching" with unprecedented precision.

One new feature that is enabled by the installation of the foils on the cathode is the completely new ability to use scintillation light to reconstruct the position in the drift using scintillation light only. This is based on the assumption that the LDS has active elements sensitive to only direct VUV light or only re-emitted visible light. The current design of the SBND system has this feature, thanks to additional PMTs not coated with TPB, which will be sensitive only to visible light. The difference between the arrival times between the VUV and visible light components can be used to unambiguously determine the position of a charge deposition with a resolution of up to 12 cm, see Fig. 5. This enables an additional handle to reject non-beam backgrounds missed by the CRT. It also provides much better precision in tagging non-beam events.

2.3 Effects on Trigger and Scintillation Time Constants.

Rayleigh scattering effects manifest themselves in the timing plots by changing the reconstructed decay time of the fast component, the further the distance traveled by the light the longer the effective decay time of the light that we measure, see Fig. 6. **This means that a typical trigger configuration which uses a fixed amount of time to gather the fast component will gather a different fraction of it depending on the distance from the PMTs.** This compounds with the non-uniformity of light collection caused by the geometric effects. As can be seen in Fig. 6 this effect is somewhat mitigated when foils are installed, as the visible component begins to dominate at long distances, and since the photons get downshifted quickly on the cathode the Rayleigh scattering effects become less significant.

2.4 R & D for DUNE

DUNE has just formed consortia to construct elements of the far detectors. The Photon Detection System (PDS) Consortium for the single phase is in the process of defining the final design of the

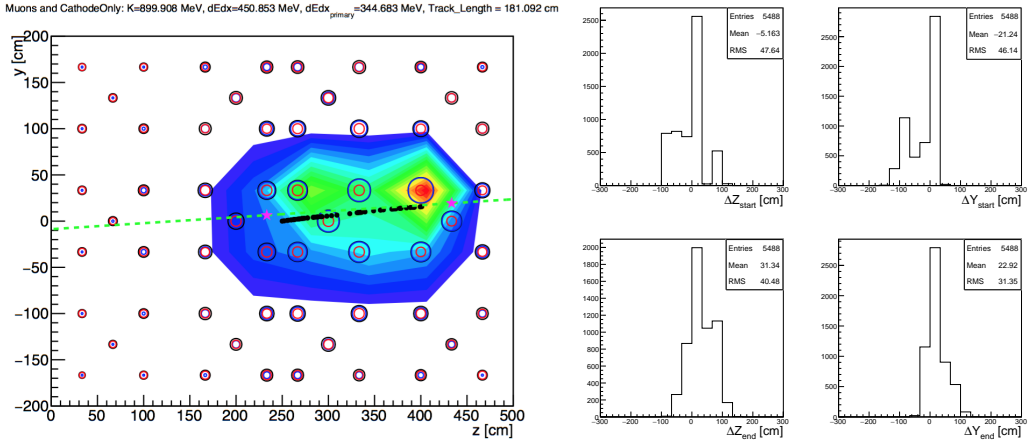


Figure 4: Left: Footprint of the light signals in the photocathode plane generated by a *cosmic* (~ 1 GeV muon) in a geometry with a cathode covered by TPB-coated reflector foils. Each circle represents the position of one PMT, and the size of the circles are proportional to the log of the signals: total (black), VUV (blue) and visible (red). The contour has been defined by the "hottest" PMTs containing the 50% of the total light. For a rough estimation of the direction of the track, a linear fit to the contour is done (dashed green line). By comparing the edges of the contour with the fit we compute the *start/end* points of the *cosmic* (pink stars in the figure). Right: Resolution in the estimation of the (z, y) *start* (top) and *end* (bottom) points for a sample of *cosmics* (~ 1 GeV muons) with different topologies. The results when using the VUV or the visible components are very similar [20].

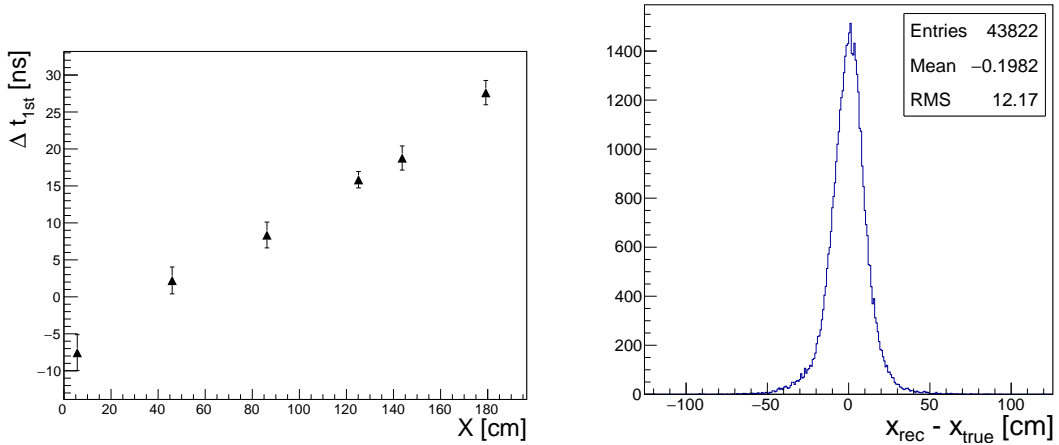


Figure 5: Difference in arrival times between direct and WLS reemitted light in with foils covering the cathode plane. The clear linear dependency allows reconstructing the X-position of the event using scintillation light (left) and the 1D resolution of reconstructed vs true position (right) [20].

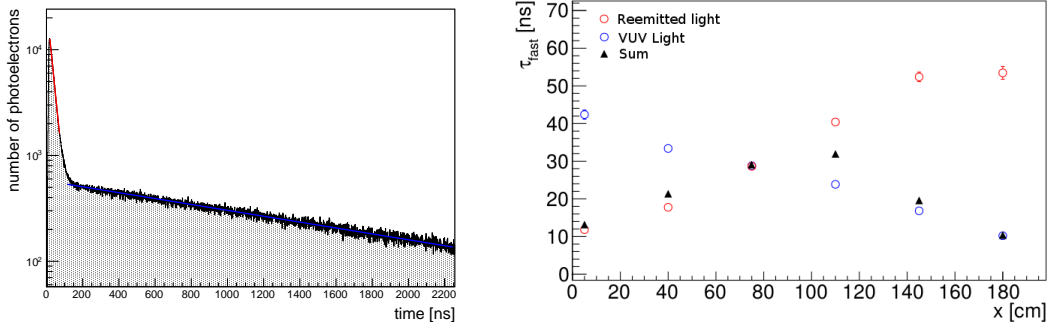


Figure 6: Left: Average VUV signal, detected by a PMT, coming from energy deposited at 100 cm from the PMTs. The decay time of the fast component is longer than expected for argon emission times caused by the convolution of the argon scintillation ($\tau_{fast} = 6$ ns and $\tau_{slow} = 1590$ ns in our simulations) and propagation (direct transport and Rayleigh scattering) times. Right: The resulting effective decay times of the fast light component reaching the PMTs have a new time structure. This modifies the original *pure scintillation* time structure of the signals, especially the fast component, in the way shown in the figure on the right, as a function of the distance to the PMT. The light components are as follows: VUV (blue), visible (red) and total (black) [20].

light collection system. One of the proposed options is now the combination of the ARAPUCA detectors with WLS-covered reflector foils, and testing the performance of such foils as well as developing their production methods are deliverables of the PDS consortium. This means that installing WLS-covered foils, apart from the physics benefits described before, can provide important input into the design of the DUNE detectors.

3 WLS-covered foils in SBND

This section describes the components and procedures proposed to manufacture the WLS-covered foils and to install them in the SBND CPA.

3.1 Substrate Foils

Given the size of CPA windows (1.20×1.00 m), a reasonable solution is to use four 50×60 cm foils per window for a total of 38.4 m 2 in 128 pieces. This is a reasonable compromise between the number of evaporation and the size of the evaporator chamber. It also necessitates obtaining large enough substrate foils. We considered two possible options, both produced by 3M: VIKUYITY[1] (also called Enhanced Specular Reflector, or ESR) and DF2000MA lighting foils[2].

3M VIKUYITY, commonly used in reflective surfaces for cell-phone displays, is a thin organic multilayer material that exhibits between 98% and 100% total reflectance for visible wavelengths above 400nm on both sides of the foil, as shown in Figure 7; diffuse reflectance contributes less than 5% of the total reflection at all wavelengths. VIKUYITY sheets are available off-the-shelf in $17'' \times 17''$ sizes, which is not sufficiently large enough for our purposes. However, 3M is also able to produce these foils in 70×70 cm sized sheets with a lead time of 7 weeks at a substantial mark-up.

3M's DF2000MA, which is commonly used as a reflecting surface for high-efficiency commercial and industrial lighting applications, is sold in rolls of 1 m width by many industrial suppliers, including Digikey, with short lead-times. The optical properties of DF2000MA are nearly identical to those of 3M VIKUYITY, as shown in Figure 7; DF2000MA exhibits diffuse reflection at about 3% or less of the total for all wavelengths, slightly below that of VIKUYITY. The primary difference between the two products is that DF2000MA serves as a 1-sided reflecting surface with an acrylic-based adhesive backing. In addition, DF2000MA is sold at a significantly reduced price compared to VIKUYITY. Both DF2000MA and VIKUYITY are sold with protective layers over their reflective surfaces.

The IIT group has significant prior experience with the DF2000MA option, as it was been utilized as the primary specular reflector in the PROSPECT detector's target segmentation system, which was fabricated in 2016-2017 at IIT by Prof. Littlejohn's research group. Moreover, the IIT

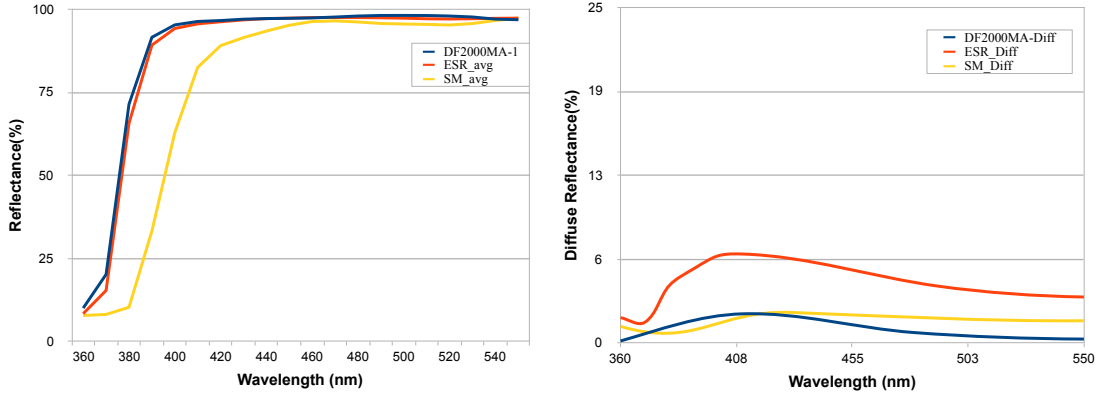


Figure 7: Left: total reflectance of DF2000MA and VIKUYITY (called ESR here) organic specular reflecting foils; also pictured for reference is SolarMirror, a high-quality metallic specular reflector. Right: diffuse reflectance for these same three foil materials. These reflectance measurements were performed by IIT as part of PROSPECT R&D.

group has a significant remaining excess of DF2000MA left over from PROSPECT production, which, if used, would account for about 1/4 to 1/2 of the needed foil material for SBND. Following positive results of R&D tests described in Sec.5.2 below, and given its low price and immediate availability at IIT, we have decided to choose the DF2000MA option.

3.2 Lamination on FR4

The adhesive on the back side of the DF2000MA foils enables lamination of the foil material onto many different substrate types. In the case of the PROSPECT experiment, 0.75 mm-thick double-sided glossy carbon fiber was utilized as a substrate, with DF2000MA laminated to both sides, as shown in Figure 8. For SBND, where foils will serve no mechanical/structural function, the range of acceptable substrates is larger, with the best substrate determined by cost, available thickness, and quality of lamination. FR4, a resin-impregnated fiberglass material similar to G10 that is most commonly used in printed circuit boards, matches all of these requirements, and has been used in R&D tests for SBND.



Figure 8: Left: Appearance of an optical reflector panel made for PROSPECT utilizing a procedure and reflector foil identical to that proposed for use in SBND. Right: appearance of the lamination setup used in PROSPECT, which is nearly identical to that proposed for use in SBND. In this picture, a double-sided adhesive is being laminated onto a DF2000MA foil that has already been laminated onto its carbon fiber substrate.

Prototype SBND reflector foils were produced by laminating 3M DF2000MA material onto both sides of a 0.032" thickness FR4 sheet that were pre-cut via CNC machine to the shape specified by

SBND mechanical drawings, which will enable them to fit into the existing CPA subframe design. Lamination is performed in a cleanroom at IIT utilizing a 26"-wide industrial laminating machine. The highest-quality laminations done for SBND R&D (free of air bubbles and wrinkling) have been achieved using two IIT undergraduate workers with significant prior lamination experience in PROSPECT. An example of the lamination setup as utilized in PROSPECT can be seen in Figure 8; the only difference between the pictured setup and the SBND case is the substitution of the pictured laminator with a wider one of the same make. Substrate sides are laminated one-by-one, with each side's lamination taking approximately 1 minute. Following lamination of both sides, Exacto knives are used to remove any excess material (in bolt holes, around edges, etc.)

One of the six produced prototype reflector foils can be seen in Figure 9, along with a technical drawing of the substrate/foil shape [24]. The process of procurement, cutting, and fabrication for these six reflectors took approximately two weeks. In addition, small prototype squares were also produced and sent to Manchester to test the resilience of the lamination to LAr dunking; no problems were observed.

As the reflector foils performed as expected, we would plan to use the same materials and procedure for fabrication of production reflector foils. We estimate that it would take approximately 1 to 1.5 months of IIT undergraduate and postdoc work to produce a full set of reflector foils ready for TPB evaporation.

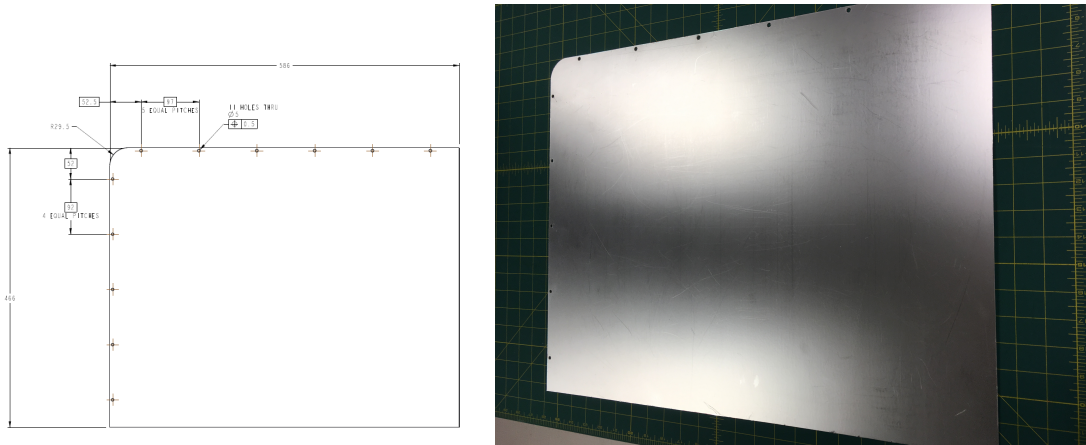


Figure 9: (Left) Technical drawing of a foil + FR4 element shape. (Right) a laminated element manufactured at IIT.

3.3 Evaporation

The foil+FR4 elements will be evaporated in two custom made evaporator chambers capable of evaporation of 60×60cm elements. There are two identical setups - one at the University of Manchester, Fig. 10, and one at UNICAMP. The Evaporation procedure has been developed for the WArP experiment and is as follows for the SBND 50×60cm FR4+foil elements:

1. Crucible located at 30cm from centre of the chamber is filled with 5g of TPB.
2. Foils are mounted to a metal disk which is appended inside of the evaporator chamber. Protective layer is removed.
3. Chamber is closed and pumped down to a pressure of 5e-5 mbar.
4. Crucible heating is turned on, and when it reaches 220°C the Crucible shutter is opened.
5. at 200°C the deposition monitor and the rotating motor are turned on.
6. once the deposition sensor ceases to show activity, see Fig. 11, the crucible heating, motor and vacump pump are all turned off.
7. vacuum is broken using nitrogen from a connected bottle to avoid condensation from water in air.

8. the procedure is repeated for the other side of the FR4+foil element.
9. The foils+FR4 elements will be sealed in plastic bags filled with gaseous nitrogen, to avoid foil deterioration during shipping.

This procedure has been developed and used for the evaporation of foils in the WArP detector as well as for the foils used in the LArIAT detector. It ensures a good quality of the deposition and a thickness of roughly $300 \mu\text{g}/\text{cm}^2$ of TPB, which has been shown to be an optimal range [19]. Sec. 5.5 describes how we predict the thickness of the TPB deposited on the foils and the method we used to calibrate it.



Figure 10: (Left) The evaporator chamber installed at the University of Manchester. The six CF63 closed off holes can be filled with crucibles in two configurations - at 15cm and 30cm. On the left of the chamber is the opening for the Turbo pump and the two rods with the deposition sensor. (Middle and Right) Foils evaporated as one of the test evaporation.

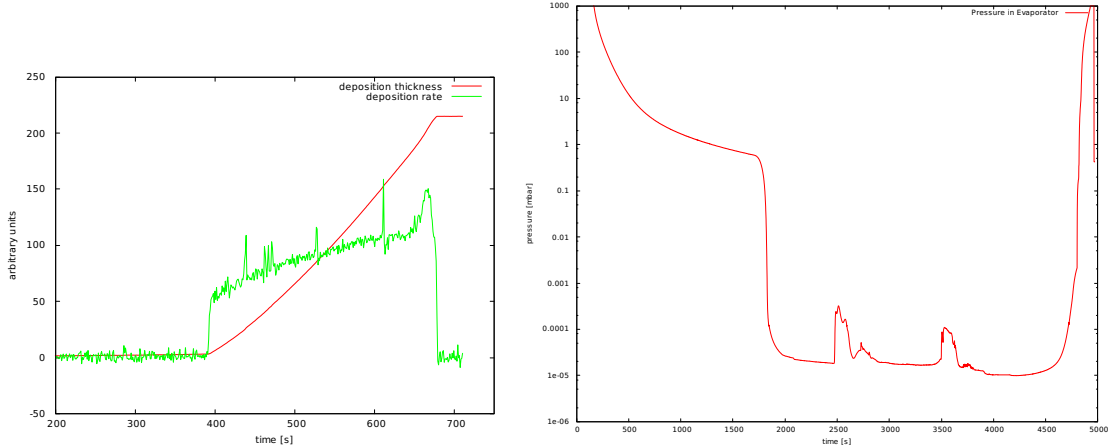


Figure 11: A readout of the deposition sensor during an evaporation (left). Green line is the deposition rate, whereas the red line is the integrated deposition thickness. The units on the axis are arbitrary, however the start and end of the evaporation can be clearly identified. (right) A time evolution of the pumping of the Manchester evaporator system during an evaporation. In this particular case the entire pumping + evaporation procedure took less than 2 hours. The two bumps occurred when turning on and off the crucible heaters, and are attributed to a glitch in the new GUI software that was being tested (pressure sensor was closed off with a valve).

3.4 Installation in the CPA

The foil+FR4 elements will be installed in the CPA. A test installation has been performed using the test frame setup at Liverpool by the Liverpool group [23]. The prototype elements manufactured at IIT have held well during the mesh-tightening procedure using liquid nitrogen. However significant condensation has been observed on the TPB surfaces when warming up after the LN_2 dunking, see Fig. 12. One possibility to avoid this effect would be to vent the cooled area with a dry gas to avoid condensation. To maintain a high performance of the foils it would be preferable to perform the foil+FR4 element installation as late as possible, ideally just before the CPA is

installed in the cryostat at Fermilab. The Liverpool group is devising an alternative tensioning method using a table with a jig, that could be used to tension the mesh without using liquid nitrogen and could be shipped to Fermilab [21].

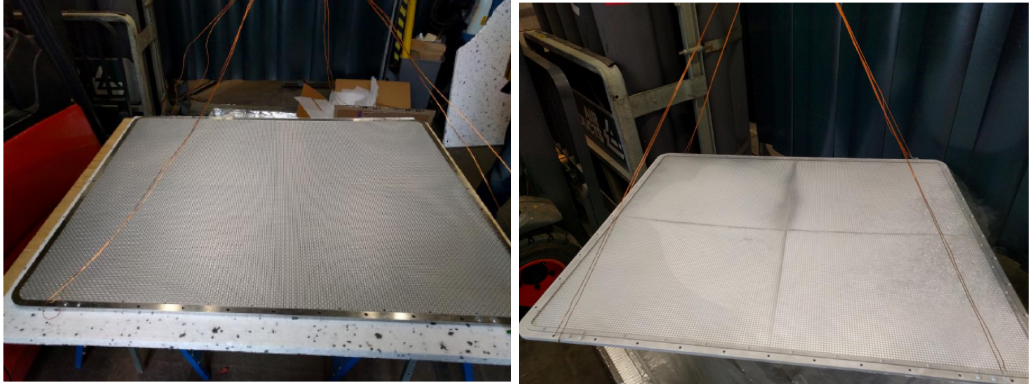


Figure 12: The test FR4+foil element installation on the Liverpool testframe [23]. (left) the four FR4+foil elements sandwiched by the mesh before tensioning. (right) after tensioning using the LN2 method.

3.5 Quality Control

To ensure that quality of evaporation is stable we will use a method developed for WArP[14] and used by DEAP[25] shown in Fig. 13. We will use a chamber observed by a PMT sensitive only to visible light. The chamber will be closed off by a small piece of foil evaporated together with the FR4+foil piece being examined. The chamber will be flushed with argon gas which scintillates in the VUV. An alpha source will produce ionizing radiation, which will be only observed at the PMT if it is converted at the small test foil covered with TPB. The Light Yield (LY) of the system corrected for impurities calculated from the tail of the light signal[5] gives an estimate of the quality of evaporation.

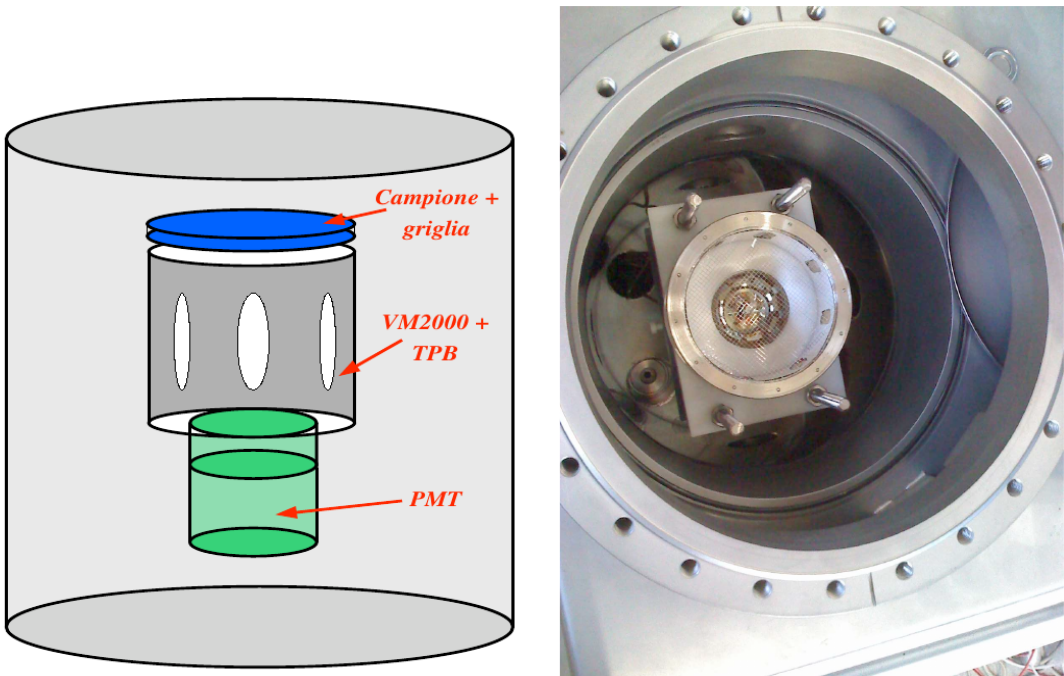


Figure 13: Small chamber used to test quality of evaporation. (Left) Scheme of operation, (Right) Photo of original chamber whilst assembled at Gran Sasso.

4 Resources

The manufacture of the foils will be performed in two steps. First the DF2000MA foils will be laminated on 0.032"-thick (0.8mm) FR4 sheets by the IIT group. The FR4 sheets with foils on both sides will then be sent to Manchester and UNICAMP for evaporation. The $4 \times 16 = 64$ FR4 elements will be manufactured in-house by IIT based on the design provided by the Liverpool group, see Fig. 9. This design makes the elements flush with the CPA frames and facilitates installation in the frames.

4.1 Experience in Previous Similar Projects

The IIT group has experience in large scale lamination of DF2000 foils on a stiff substrate, having performed this operation for production of the PROSPECT detector's target segmentation system, as described above. The Manchester and UNICAMP have experience in large scale evaporation operations having performed them for the WArP detector VETO system. This required evaporating ~ 200 -pieces and affixing them to copper elements of the structure. See Fig. 14. Manchester has recently performed the evaporation of the additional foils installed in LArIAT described in Sec. 5.1 getting experience with the new, larger size, system. E.S. has developed the quality control system mentioned in 3.5.

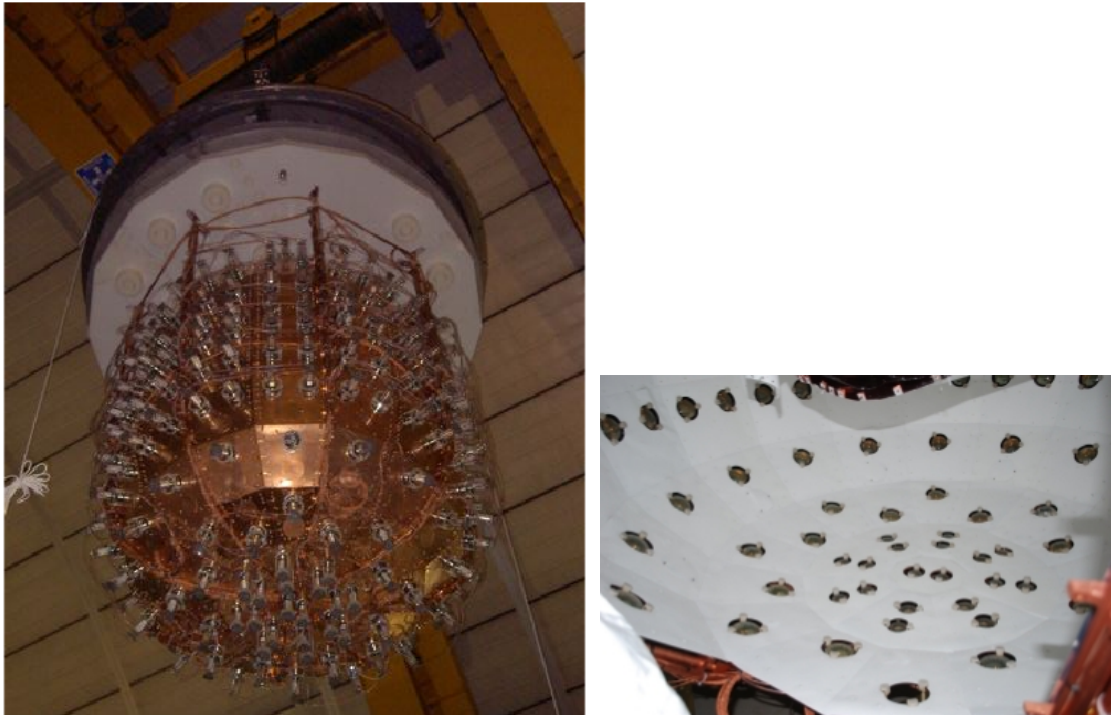


Figure 14: The WArP 100 liter external Veto (left). And a view of the bottom of the "egg" composed of tiles with evaporated di-electric foils. The area covered by TPB-evaporated foils was equal to 18 m^2 , and the evaporation lasted 3 months.

4.2 Infrastructure

The equipment needed to perform the foil production is in place. IIT has already purchased and set up an industrial laminator with the required width for prototype production [3] in an already-existing soft-wall cleanroom at IIT. Both Manchester and UNICAMP have purchased large scale evaporators, see Fig. 10. The Manchester evaporator is already operational and tested, the UNICAMP unit has been delivered and is being set-up. Both evaporators are set-up in clean rooms in the respective institutions. The small chambers to perform Quality Control measurements are being set-up. the UNICAMP machine has been transported from Italy, the Manchester unit is expected to be completed in 3-4 weeks.

4.3 Time Estimates

4.3.1 Lamination

We expect the 128 laminations to take on the order of 8 hours. CNC cutting of the FR4 substrate to the designed shape, removal of excess foil material from the substrate, and visual and optical QA will likely result in a total production time of 3-4 weeks, we conservatively estimate 1.5 months. The first set of samples could already be sent out prior to completion of all foils, meaning that the evaporation sites need not wait the full production time to begin evaporation. Furthermore, the presence of existing DF2000MA material at IIT and the short lead-time of FR4 from most standard plastics vendors would enable production to proceed within a few weeks if foils are approved for production.

4.3.2 Evaporation

A typical evaporation takes on the order of 2 - 2.5 hours depending on the experience of the team performing the task. About an hour of this is taken up by pumping down time, see Fig. 11, the rest of the time is taken by heating the crucibles, breaking the vacuum and changing the samples. An experienced team can minimize the last element and relatively easily perform 4 evaporation in a day. This leads to an estimate of 16 working days, estimated to 3.5 weeks per each site to perform the needed evaporation. This could be shortened if needed by adding a shift system and increasing the number of evaporation per day. We anticipate that the evaporation at Manchester will start before those at UNICAMP, and in case of time constraints the division of number of evaporation between the sites can be adjusted.

4.3.3 Installation

The Liverpool group has performed a test installation using prototype laminated FR4+foil elements, see [23] for details. Using their test-frame they were able to tension the mesh with the laminated pieces in a relatively short time. Such a procedure should be repeatable for the actual CPA assembly and it should be possible to install the mesh in the course of a few days. Given the collection of humidity resulting from the temperature difference resulting from dunking in LN₂ it would be preferable to perform the installation with a mechanical tensioning method instead of the thermal cycling method.

Given the sensitivity of the evaporated foils to sunlight and humidity it would be preferable to perform the installation at Fermilab just before the CPA is installed in the Cryostat rather than in the UK. In this case, the installation would be performed using a table with jig designed by the Liverpool group, which would be shipped together with the CPA. The foils would be installed in the 16 subframes removed from the CPA, using the jig to tension each of the subframes. In case the CPA will be vertical during installation, a scissor lift might be necessary. If the CPA frame was in the horizontal position, the operation could be performed without the need for a lift. In this case we estimate a week for the installation of the foils, given the yet unknown complexity of the table jig setup.

4.4 Person Power

We have sufficient person-power to perform the previously mentioned stages. IIT has 4 persons (see Tab. 1) available to perform the laminations.

Person	Position	IIT Availability	FNAL availability
B. Littlejohn	Academic	yes	yes
D. Martinez	PD	yes	yes
K. Hermanek	Undergrad	yes	no
I. Gustafson	Undergrad	yes	no

Table 1: IIT person-power for laminations and on-site installation support.

The evaporation are planned to be split into shifts of 5-6 hours. Manchester, see Tab. 2, has enough hands to form 3, possibly 4, 2-person teams. UNICAMP, see Tab. 3, has a similar number of available persons. This allows a continuous production of 4 foils per day (possibly more at later stages) and avoids overworking the production teams, keeping the number of shifts to 4 per week.

Person	Position	MCR Availability	FNAL availability
A. Szclc	Academic	yes	yes
D. Garcia-Gamez	PD	yes	yes
A. Furmanski	PD	varied	yes
C. Hill	PG Student	no	yes
D. Porzio	PG Student	yes	no
V. Basque	PG Student	yes	no
PG Student 1	PG Student	yes	no
PG Student 2	PG Student	yes	no
MCR Tech	Technician	if needed	no

Table 2: Manchester person-power for Evaporations. The Two PG students start classes, and choose project during the weeek of the 25th of September.

Person	Position	UNICAMP + UFABC Availability	FNAL availability
E. Segreto	Academic	yes	yes
A. A. Bergamini-Machado	Academic	yes	yes
A. Benvenho (UFABC)	Academic	yes	no
D. Criado(UFABC)	Academic	yes	no
A. Fauth(UNICAMP)	Academic	yes	no
B. Gelli	PG Student	yes	no
PG Student 2	PG Student	yes	no
5 x UG Student	UG Student	yes	no
UNICAMP Tech	Technician	if needed	no

Table 3: UNICAMP person-power for Evaporations.

The UNICAMP and Manchester groups have dedicated travel funds from the SPRINT-FAPESP programme that enable us to travel between the two sites, in case a shift of person power was necessary.

Should the final FR4+foil element installation happen at Fermilab, which is preferable, both Manchester and UNICAMP will send persons to perform that installation, and will be assisted by the IIT group, which is located in the area. Note that some group members are already based at Fermilab and can assist in the installation. The Manchester group members travelling to Fermilab for the installation will have been trained by the Liverpool group in the use of the tensioning jig table before travelling. Depending on the operations required we may need assistance from Fermilab technicians during the installation.

4.5 Costs

The material costs of manufacturing the elements which are the object of this proposal are listed in Tab. 4. There have been additional costs, mostly to prepare the infrastructure needed for the manufacturing, such as the laminator machine, or the evaporators and the chambers for quality control. As these costs have already been made, we have excluded them from this proposal. This leaves a cost of on the order of 15k\$. We propose to cover this cost from our respective start-up funds and request no funds from the project to fund these purchases.

4.6 Summary of Resources

We are ready to begin foil production. The crucial infrastructure is in place. We have the necessary person-power to perform all of the steps of the production and installation. The costs of production

Material	Amount	Cost	Lead time
TPB	640g	6000 GBP	2-3 weeks
DF 2000MA	38.4 m ²	3600GBP/62m ²	3 weeks
0.75mm Fr4	38.4 m ²	800\$	1-2 weeks

Table 4: Material costs needed to perform production.

are relatively modest, once the infrastructure is in place and we propose to cover them from our University funds. Should the final installation happen at Fermilab, we would request assistance from Fermilab technicians in case heavy lifting is required.

5 Supporting Tests and R & D

This section describes various tests and studies we have performed to show that installing WLS foils in the detector is beneficial to the detector and does not cause any negative effects (under reasonable assumptions), as well as supporting measurements and/or calibrations performed to understand the production process.

5.1 The LArIAT Runs

The most important proof of principle of using foils to enhance the light collection efficiency in a liquid argon TPC comes from the long experience of running in LArIAT [27]. LArIAT has completed three full runs with a set of six TPP-evaporated VIKUITY foils placed on the walls of the field cage, see Fig. 15. The result of this was a uniform light collection efficiency and an augmented Light Yield (LY) compared to a setup with only two small PMTs observing the chamber. The light uniformity, as seen in Fig. 16 has been predicted by LArSoft and standalone simulation. Both of these have been validated by comparison with data, at the most basic level by comparing the obtained LY with expectations. See Fig. 1, left, for the standalone and Fig. 16 for the LArSoft simulations. The results and experience from running LArIAT have been incorporated into the SBND simulation system presented in [20].

The LArIAT runs provide invaluable experience in exploiting a neutrino-energy detector with TPB covered reflector foils installed inside. The PMTs in LArIAT were not coated in TPB through most of the data taking, which means that almost all of the registered light is the downshifted visible light. The fact that scintillation light was observed throughout all three runs means that the foils continued to be effective for three years, thanks to the precautions taken when opening the detector. Namely, humidity and direct sunlight was avoided, most often by covering all of the ports of the cryostat by a sealed tarp during non-data taking periods. No major deterioration of the foils was observed leading to the conclusion that the evaporation method we propose results in mechanically stable foils. The one significant difference between most of the LArIAT data taking runs and our proposal for SBND is the fact that the foils were not placed on the cathode, and instead on the walls of the TPC. For this reason we have performed a dedicated run with an SBND-like mesh cathode with and without foils installed in the detector. This test and preliminary results are described in the next Section.



Figure 15: The inside of the LArIAT TPC lined with foils.

5.1.1 LArIAT test run with mesh cathode

To test the functioning of a foil + mesh setup in a working detector we constructed an SBND-like cathode plane assembly in the University of Manchester physics workshop. The design was based on the SBND CPA step files kindly provided by P. Sutcliffe, Liverpool. The manufactured LArIAT cathode can be seen in Fig. 17. It contained two SBND-like window frames constructed from

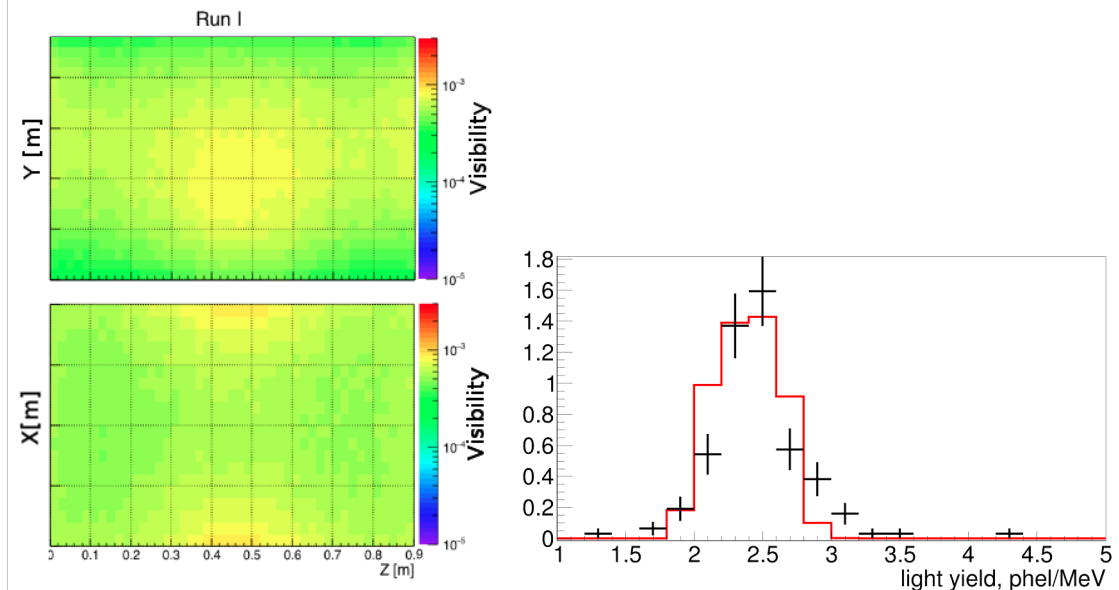


Figure 16: (left) Visibility (defined as fraction of detected photons from a given point in space) maps for the LArIAT light collection system based on a stand-alone simulation. Upper figure shows view from the side with the PMT flange in the center, while the bottom plot shows the same map viewed from the top of the detector looking down. (right) Light Yield obtained with throughgoing muons compared with the LArSoft-based simulation prediction, see Fig. 1 for data-standalone sim comparison.

stainless steel. The frames hold two layers of mesh identical to the one to be used by SBND, courtesy of the Liverpool group. The metal parts are surrounded by a 10cm G10 frame, which is needed to position the fieldcage horizontally and to isolate the cathode from the steel cryostat which is at ground. The new cathode was attached to the fieldcage using an epoxy glue. During the first phase of LArIAT run III, lasting from March to late April, the cathode was installed without foils inside. In the second part of Run III, lasting from June to July, two foils evaporated with $\sim 300\mu\text{g}/\text{cm}^2$ of TPB were installed by sandwiching the foils between the two layers of the mesh and tightening the screws. The result can be seen in Fig. 18. In both cases no negative effects of the mesh cathode nor foils installed in the mesh cathode were observed. A net improvement of light yield was observed, on the order of 20%. The relatively small increase results from a combination of three effects: first, the inside of the TPC is already lined with foils, so a day/night scale of effect is not expected. Second, the wire pitch in Run IIIb is 3 mm, compared to 5mm in Run IIIa, meaning the wires can block more light in the later run. Finally, the number of available electronics channels necessitated adding a wall of G10 in the wire plane side of the TPCs in the 3mm configuration, see Fig.17 which can block a fraction of the light. A more precise evaluation using an updated version of the MC Geometry is in progress.

In summary, we have demonstrated that a LArTPC can run successfully with WLS-evaporated foils in the mesh cathode for prolonged periods of time.

5.1.2 Using LArIAT data to understand Ion Recombination in Argon

MicroBooNE has been observing a, still unexplained, excess of scintillation light noise events. There are several possible explanations that are on the market, a few of which involve the positive ions that are freed during ionization events. These positive ions are then drifted towards the cathode, and could in principle recombine either on the way or as they arrive at the cathode [17]. Should a mechanism exist for the ions to recombine at the cathode with emission of scintillation light, the number of light noise events resulting from these ions could be significantly higher than in MicroBooNE. One should note though that even in this case, the total amount of light cannot be larger than double of the light emitted during the initial particle interactions, given that at 500V/cm, the deposited energy is split roughly evenly between prompt scintillation and drifting charge. The late light will be proportional to the drifting charge.

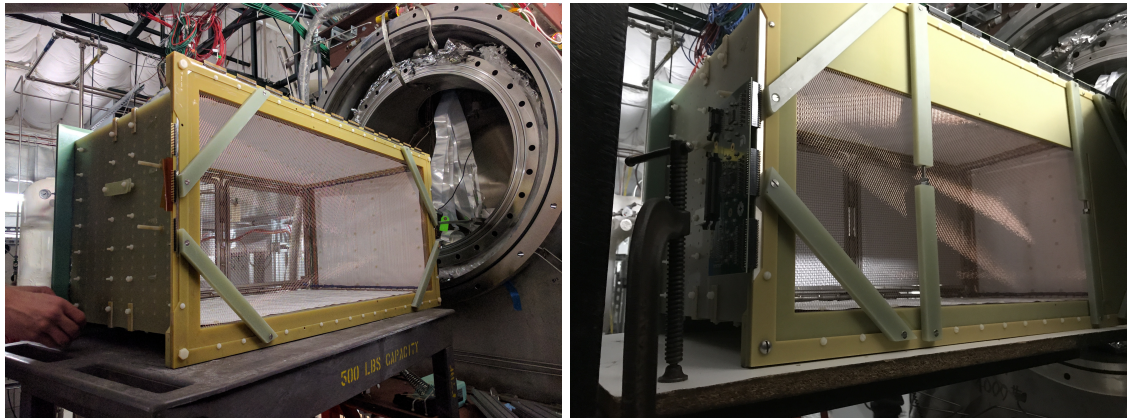


Figure 17: The LArIAT TPC with an SBND-like mesh cathode installed (left). The front view of the TPC in the second part of RunIII, where TPB-evaporated foils were installed in the cathode (right). Note the G10 plates limiting the view size of the PMTs.



Figure 18: The LArIAT Cathode with foils installed, closeup. The foils previously installed on the fieldcage walls can be seen in the background.

The ion drift velocity is of the order of 8mm/s which means that in LArIAT an ion would drift the whole width of the chamber in about one minute, which corresponds to the length of one beam cycle. This makes LArIAT an ideal location to search for patterns in delayed scintillation light from charge depositions. We have taken several sets of dedicated runs looking at random light noise in the waveforms at different tertiary beam intensities, and field strengths in the chamber. At first approximation if the light noise is a result of recombining ions then its intensity should grow with electric field strength as more ions are dragged away from the interaction site. If the scintillation results from the standard scintillation type, the dependence should be opposite, as the light quenching grows with E-field.

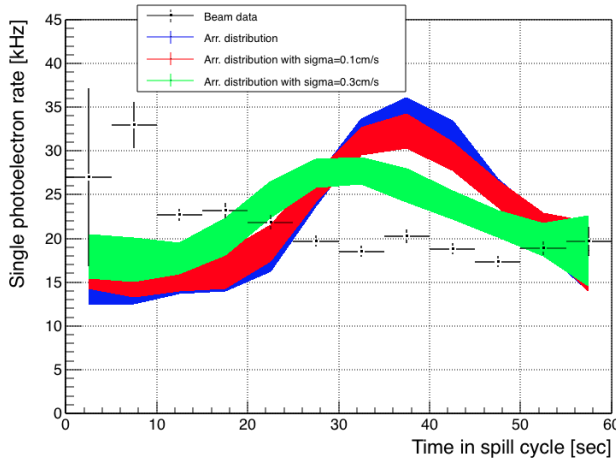


Figure 19: An overlay of “light noise” over sixty spills (1 hour) acquired during a dedicated LArIAT pulser run (black points) with the expecations of a model assuming that the charge deposited by particles in frames triggering the beamline drifts and emits light at the cathode. Three models are shown: no diffusion (blue) 0.1 cm/s (red) and 0.3 cm/s (green).

We have observed a dependency of scintillation light noise rate with the amount of charge deposited in the chamber in a beam spill. We have also observed that the light noise can be decomposed into two components: one consistent with a random distribution and one consistent with liquid argon scintillation light. The latter is unlikely to be a result of ion recombination. We have performed a cursory study, using simulations of the LArIAT beamline, which predict the shape the beam energy deposition has in the TPC. We took these energy depositions and propagated them towards the cathode with a velocity corresponding to the positive ion drift. This allows performing a cursory shape analysis to test whether recombination at the cathode recovers the shape observed in data. The result of such a simple study is shown in Fig. 19. The black points represent the rate of single photoelectrons found, averaged over the spill cycle. The MC is composed of a dedicated Corsika simulation to account for the cosmic component and a beamline component to account for the charge injected during the beam spill (0 - 4 seconds in Fig. 19). The cosmic MC was normalized using the rate obtained during a cosmic only pulser data run in the same conditions. The additional counts in MC resulting from beam were then area normalized to the additional data counts in the beam + cosmic data sample.

This simple study seems to show that light coming from ions recombining at the cathode is not preferred by the data. Our preliminary studies seem to instead imply that the positive ions might recombine on their way to the cathode and therefore emit light mostly located in the centre of the detector. Should that be the case that would provide an additional source of light noise which **will may be more difficult to calibrate out if no foils are installed in the detector** given the non-uniformity of the light collection efficiency in the chamber.

5.2 Effect on argon purity - Material Test Stand

One of the possible effects of putting dielectric foils with an adhesive into the detector would be the loss of electron purity due to electronegative contaminations. To ensure that the foils we are planning to use do not cause this effect we have asked to test them in the Material Test Stand

at Fermilab [11]. DF2000MA, DF2000MA laminated on FR4 and VIKUITY samples have been tested. Here, we present the results of the sample of the DF2000MA with the adhesive in the back. The plots can be seen in Fig. 20 and the full file results can be recovered from the LArTPC DocDB [4].

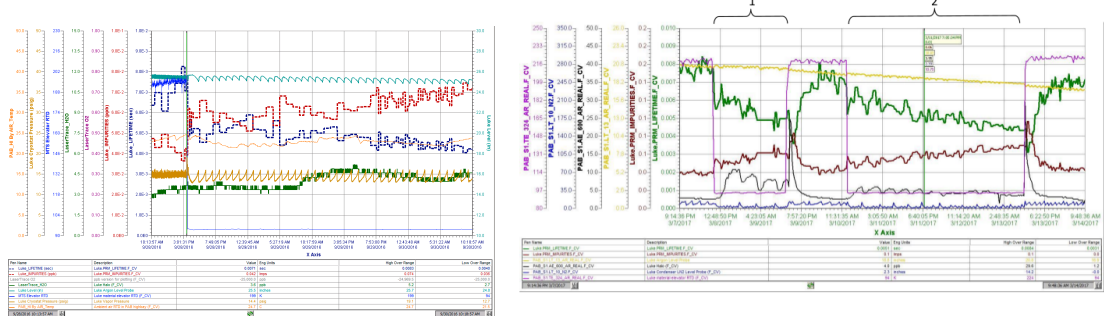


Figure 20: Results from a "zero" run of the MTS (left) and the run with the DF2000 adhesive backed foils (right). Both samples plateau at 4ms, which suggests that the DF2000 sample does not have a negative impact on electron purity.

These results can be interpreted as follows: in the test of the DF2000MA foil as well as the VIKUITY foils the nominal lifetime flattened out at ~ 4 ms. This is consistent with the most recent empty run, as well as a recent test of a set of brass nuts (metal is not expected to have any influence on purity), in which case the lifetime also flattened out at about 4 ms.

In the opinion of the MTS experts, the foils are not having any major (=detectable) impact on the liquid purity. Which should be understood as an immediate impact on lifetime that drops far below what is seen during zero tests [8].

Given these results we have chosen to pursue the more economical DF2000MA foil option rather than the more expensive, non-adhesive based VIKUITY, especially since it allows us to laminate on the FR4 substrates making them stiffer and more resilient.

5.3 Mitigation of ^{39}Ar Light Backgrounds

An important aspect of a high LY PDS in liquid argon is that low energy backgrounds can generate a large quantity of light in the detector and possibly overwhelm the signals in the detector. The most abundant low energy background in liquid argon detectors is the argon itself, namely its isotope with the mass number of 39. ^{39}Ar is a β -emitter with an endpoint energy of 562 keV and an abundance of 1Bq/kg in the liquid [13].

We have performed a study on possible cuts to remove all events stemming from ^{39}Ar events in the PMTs and what their effects would be on the spectrum of potential supernova neutrino interactions in the detector. Supernova neutrinos were used as their energy spectrum is only on order of magnitude removed from ^{39}Ar . Our findings are described in an SBND technical note: [16], however, we present a few highlights of this study.

In the study we simulated single ^{39}Ar events to test the effects of straight energy overlap as well as full frames with ^{39}Ar events to test the pileup. An example of the first case is shown in Fig. 21 where sample cuts are used to completely suppress light triggers coming from ^{39}Ar without affecting the spectrum of neutrinos from a supernova. Once we introduce overlap, the method to gauge the backgrounds introduced by ^{39}Ar is to count the time between triggers due to backgrounds. This is shown Fig. 22 (left), where we can see that in the case of a configuration with no-foils the time between triggers is the longest for given set of cuts - this is due to the lower quantity of light. However, once we look at the efficiency detection, Fig. 22 (right), demonstrates the trade-off for this as, the efficiency in the no-foils case becomes much lower than for the foils on the cathode case.

5.4 Saturation Studies

The additional amount of photons observed in the PMTs from the reflected, wavelength-shifted light could in principle cause saturation effects. We have tested this using a simple model of the

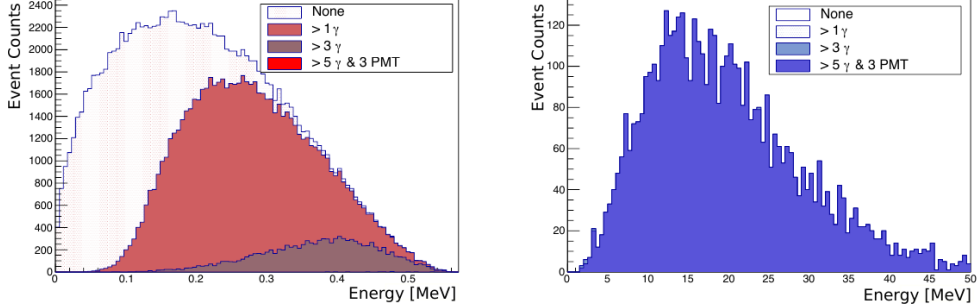


Figure 21: Energy spectra for ^{39}Ar and supernova neutrinos, assuming a large statistics sample for both, to observe how cuts on the number of photoelectrons per a number of PMTs modify the spectra. This case assumes reflective foils, considers the contribution from both direct VUV and reflected visible light, and replicates measuring only the “fast” light component by accepting only photoelectrons measured in the first 100 nanoseconds [16].

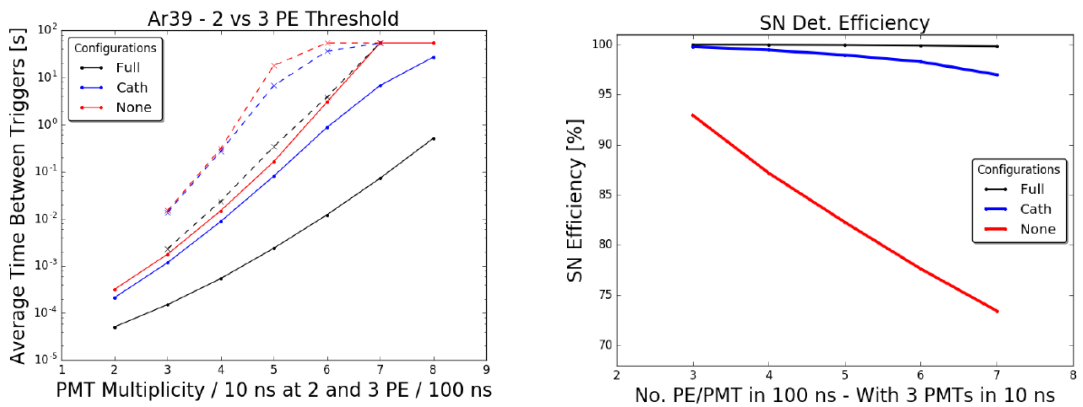


Figure 22: (left) Comparison of PMT multiplicity cuts to increase average time between triggers induced by ^{39}Ar . Dotted lines represent the case where the PMT thresholds are each set to 3 photoelectrons, and the solid lines 2 photoelectrons. The colour of the line indicates PDS configuration. “cath” is used to describe the configuration with foils on the cathode, “none” a set-up without foils. (right) Efficiency of threshold detecting photoelectrons produced from a supernova neutrino event as a function of the number of photoelectrons required on a PMT, given a 3 PMT case [16].

PMT electronics system, i.e. assuming a photoelectron width of 10ns we simulated signals arriving at each PMT for charged muons with energies from a 100 to 500 MeV of Energy. We then plotted the fraction of PMTs that are saturated for a given distance from the energy emission. We found that quite a large fraction of PMTs will be saturated if the energy deposition is relatively close to the PMTs. This effect is however intrinsic to the direct VUV light and the Visible light seems to arrive significantly diffused in time as to not cause saturation even when it is the dominating component of arriving light (high-X) values. This is visually presented in Fig. 23.

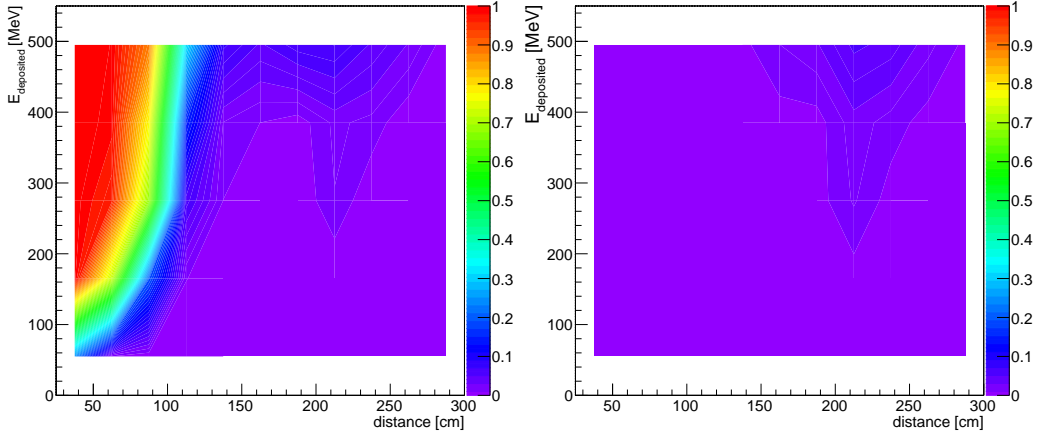


Figure 23: A study of saturation effects expected in the PMTs from all of the light (left) and only visible light (right).

5.5 Evaporator Calibration

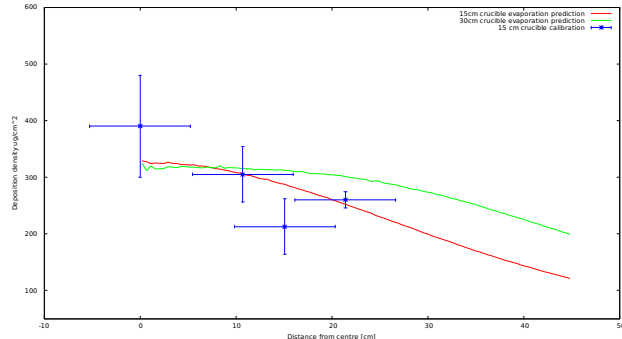


Figure 24: Preliminary calibration of the Manchester evaporator. Red line is the prediction of the simple toy MC predicting the deposition thickness and the blue points are the results of a measurement made by weighing substrate foils before and after. The green line shows the prediction of the Toy MC for a different crucible which results in a much more uniform deposition throughout the chamber, and which would be used for the SBND evaporation.

Throughout this document we have assumed that the foils will be installed with a thickness of $\sim 300\mu\text{g}/\text{cm}^2$. The deposition thickness is a function of the amount of TPB placed in the crucible, the position of the crucible in the chamber and the chamber geometry. To translate the amount of TPB placed in the crucible to a deposition thickness we used a dedicated piece of simulation code developed for the WArP experiment and its evaporator. To ensure that the simulation works also for the new larger chambers recently installed at Manchester and UNICAMP, we are performing a few dedicated calibration runs.

In these runs we place smaller pieces of di-electric foils at well defined places on the substrate disk. Before this we weigh them without the protective covers on a precision scale closed in a box to avoid air drafts and wrapped in aluminum foil to minimize electrostatic effects. The foils

are then evaporated and weighed again in the same way as before. The difference in weight is attributed to the TPB deposited on the foil. Given the placing of the foils we have 3 sets of 4 foils at 3 different radii and one central piece. This allows us to average the deposition width for the outer pieces and compare the results (blue points) with the predictions (red line) in Fig. 24. The agreement is reasonable, which means that the foils are being evaporated with the expected thickness. For reference, we show the green line, which is the deposition thickness expected for an evaporation with a crucible placed at 30cm, which will be the configuration used for the SBND foil evaporation as it provides more uniformity further away from the centre.

6 Conclusions

Through an extensive simulation program we have demonstrated that the installation of WLS-coated reflector foils in the SBND CPA assembly will be beneficial to the experiment’s physics goals by ensuring a more uniform light collection. This in turn will translate into the capability to use scintillation light for calorimetry, especially for events at lower energies, as well as improved timing and position reconstruction. Adding the new component of light, reflected off the foils placed on the cathode will enable a completely new feature in the detector, namely the ability to reconstruct the X-position of a light flash in addition to its Y-Z position. This will translate into more efficient signal finding and therefore better background suppression. We have performed dedicated studies and measurements which do not show any effects that look detrimental to the functioning of the detector.

We therefore propose to manufacture a set of TPB-evaporated di-electric reflector foils laminated on thin FR4 sheets. We have the necessary infrastructure and resources to produce this enhancement to the SBND detector. Our groups also have experience in producing almost identical systems on similar scales, which ensures a smooth operation.

We believe that this addition to the SBND detector will enhance its performance and broaden the physics programme as well as its R&D programme for future large-scale liquid-argon detectors like DUNE. Given approval, we are ready to begin production within a very short time frame.

References

- [1] 3M VIKUITY foils. <https://en.wikipedia.org/wiki/Vikuiti>. Accessed: 2017-09-20.
- [2] DF2000 specular reflector. <https://www.digikey.co.uk/product-detail/en/3m/75347099659/75347099659-ND/4988904>. Accessed: 2017-09-10.
- [3] Drytac JetMounter 25". https://www.usi-laminate.com/store/wpbec_viewItem.asp?idProduct=3594&search=jetmounter&go=. Accessed: 2017-09-20.
- [4] MTS test stand measurement of df2000. https://lartpc-docdb.fnal.gov/cgi-bin/private/RetrieveFile?docid=465&filename=Material_Test_Reflective_Film_all.pdf&version=7. Accessed: 2017-09-10.
- [5] R. Acciarri et al. Effects of Nitrogen contamination in liquid Argon. *JINST*, 5:P06003, 2010.
- [6] R. Acciarri et al. Design and Construction of the MicroBooNE Detector. *JINST*, 12(02):P02017, 2017.
- [7] R. Acciarri et al. Michel Electron Reconstruction Using Cosmic-Ray Data from the MicroBooNE LArTPC. *JINST*, 12(09):P09014, 2017.
- [8] Alan Hahn. Private communication.
- [9] T. Alexander et al. Light Yield in DarkSide-10: A Prototype Two-Phase Argon TPC for Dark Matter Searches. *Astropart. Phys.*, 49:44–51, 2013.
- [10] S. Amerio et al. Design, construction and tests of the ICARUS T600 detector. *Nucl. Instrum. Meth.*, A527:329–410, 2004.

- [11] R. Andrews, W. Jaskierny, H. Jostlein, C. Kendziora, S. Pordes, and T. Tope. A system to test the effects of materials on the electron drift lifetime in liquid argon and observations on the effect of water. *Nucl. Instrum. Meth.*, A608:251–258, 2009.
- [12] P. Antonioli et al. SNEWS: The Supernova Early Warning System. *New J. Phys.*, 6:114, 2004.
- [13] P. Benetti et al. Measurement of the specific activity of ar-39 in natural argon. *Nucl. Instrum. Meth.*, A574:83–88, 2007.
- [14] P. Benetti et al. First results from a Dark Matter search with liquid Argon at 87 K in the Gran Sasso Underground Laboratory. *Astropart. Phys.*, 28:495–507, 2008.
- [15] F. Cavanna, M. Kordosky, J. Raaf, and B. Rebel. LArIAT: Liquid Argon In A Testbeam. 2014.
- [16] Colton Hill, Andrzej Szelc, Diego Garcia-Gamez. Suppressing low energy background scintillation signals in sbnd. *SBN-DocDB*, (#1574), 2017.
- [17] R. V. de Water. Positive ion drift and foil option. *SBN-DocDB*, (#1065), 2016.
- [18] W. Foreman. Light-Based Triggering and Reconstruction of Michel Electrons in LArIAT. *JINST*, 11(01):C01037, 2016.
- [19] R. Francini et al. VUV-Vis optical characterization of Tetraphenyl-butadiene films on glass and specular reflector substrates from room to liquid Argon temperature. 2013.
- [20] Garcia-Gamez, D. and others. Light detection system simulations for sbnd. *SBN-DocDB*, (#1155), 2017.
- [21] Kostas Mavrokordis. Private communication.
- [22] A. Mirizzi, I. Tamborra, H.-T. Janka, N. Saviano, K. Scholberg, R. Bollig, L. Hudepohl, and S. Chakraborty. Supernova Neutrinos: Production, Oscillations and Detection. *Riv. Nuovo Cim.*, 39(1-2):1–112, 2016.
- [23] D. Payne. CPA Cold Tests. *SBN-DocDB*, (#3263), 2017.
- [24] Peter Sutcliffe. Private communication.
- [25] T. Pollmann, M. Boulay, and M. Kuzniak. Scintillation of thin tetraphenyl butadiene films under alpha particle excitation. *Nucl. Instrum. Meth.*, A635:127, 2011.
- [26] K. Scholberg. Supernova Signatures of Neutrino Mass Ordering. 2017.
- [27] A. M. Szelc. The LArIAT light readout system. *JINST*, 8:C09011, 2013.